11th Paper_Nurhasni Hasan (2018).pdf

by

Submission date: 14-May-2023 09:24AM (UTC+0700)
Submission ID: 2092390667
File name: 11th Paper_Nurhasni Hasan (2018).pdf (1.84M)
Word count: 7371
Character count: 39308

Journal of Drug Delivery Science and Technology 48 (2018) 457–465

Contents lists available at ScienceDirect

Journal of Drug Delivery Science and Technology

journal homepage: www.elsevier.com/locate/jddst

In vitro and *in vivo* evaluation of MHY908-loaded nanostructured lipid carriers for the topical treatment of hyperpigmentation

Hasanul Banna[a,1], Nurhasni Hasan[a,1], Juho Lee[a], Jihyun Kim[a,b], Jiafu Cao[a], Eun Hee Lee[c], Hyung Ryong Moon[a], Hae Young Chung[a], Jin-Wook Yoo[a,*]

[a] College of Pharmacy, Pusan National University, Busan, 46241, South Korea
[b] Department of Cogno-Mechatronics Engineering, College of Nanoscience and Nanotechnology, Pusan National University, Busan, South Korea
[c] College of Pharmacy, Korea University, Sejong, South Korea

ARTICLE INFO

Keywords:
Anti-melanogenesis
Tyrosinase inhibitor
MHY908
Nanostructured lipid carrier
Topical drug delivery

ABSTRACT

Hyperpigmentation disorder, caused by the immoderate performance of tyrosinase, is a major abnormality of human skin. Downregulation of tyrosinase enzyme through tyrosinase inhibitors has emerged as an effective strategy for hyperpigmentation therapy. In this study, a newly synthesized tyrosinase inhibitor (MHY908) was loaded into a nanostructured lipid carrier (MHY908/NLC) for the topical treatment of hyperpigmentation. MHY908/NLCs were prepared by a reverse instilling technique of melt and ultrasonication. Differential scanning calorimetry (DSC), X-ray diffraction (XRD), and transmission electron microscopy (TEM) analysis showed that MHY908 was highly dispersed and encapsulated in NLC in an amorphous state. MHY908/NLCs exhibited a dual drug release kinetic (initial burst release followed by prolonged drug release), higher skin permeation, and significant occlusion effect (*in vitro* and *ex vivo*) than MHY908 solution. The anti-melanogenesis activity of MHY908/NLCs in a mouse model of UVB-induced hyperpigmentation was significantly higher than that of MHY908 solution. Furthermore, the *in vitro* cytotoxicity test revealed the non-toxicity of MHY908/NLCs to healthy fibroblast cells. Therefore, MHY908/NLC could serve as a promising topical delivery system for the treatment of hyperpigmentation.

1. Introduction

Melanin is a pigmented biopolymer synthesized by melanocytes that is encased into melanosomes and endogenously moved to the adjoining keratinocytes [1]. The packaged cutaneous pigment is then used for epidermal photoprotection and thermoregulation [2]. Melanin has gained much attention as a UV damage protectant as well as a camouflage and adornment agent in cosmeceuticals. However, excessive melanin expression in the dermis caused by hyperfunctional melanocytes may lead to several dermatological challenges ranging from nonmalignant melasma to freckles and lentigo [3–5]. To control melanin overproduction, various regulatory processes have been studied and it was found that the tyrosinase enzyme is responsible for catalyzing distinct reaction cascades in melanogenic pathways, thereby regulating melanin biosynthesis by controlling the rate-determining steps in melanogenesis [6,7]. In this regard, the inhibition of tyrosinase has been widely employed as an effective strategy to alleviate cutaneous hyperpigmentation [8,9].

A newly synthesized competitive tyrosinase inhibitor, 2-(4-[5-chlorobenzo{*d*}thiazol-2-yl]phenoxy)-2-methylpropanoic acid (MHY908), has emerged as a promising therapeutic alternative for the treatment of hyperpigmentation. MHY908 showed tyrosinase inhibition activity (IC_{50} = 8.19 μM) higher than that of kojic acid (IC_{50} = 10.33 μM), a well-known tyrosinase inhibitor widely used for the treatment of hyperpigmentation. In addition, the binding affinity of MHY908 to tyrosinase was greater than that of kojic acid [10]. While the applications of conventional tyrosinase inhibitors such as kojic acid and hydroquinone are restricted owing to their potential cytotoxicities, MHY908 attenuated the production of melanin in melanoma cells without any cytotoxicity. Despite its promising activities, however, MHY908 delivery to the target epidermic area where melanocytes produce melanin still remains challenging, owing to the presence of stratum corneum—a formidable barrier to skin delivery [11,12].

Over the last decade, nanostructured lipid carriers (NLCs) have

Abbreviations: MHY908, 2-(4-[5-chlorobenzo{*d*}thiazol-2-yl]phenoxy)-2-methylpropanoic acid; MHY908/NLCs, MHY908-loaded NLCs

* Corresponding author. College of Pharmacy, Pusan National University, Busan, 609-735, South Korea.
E-mail address: jinwook@pusan.ac.kr (J.-W. Yoo).

[1] These authors are equally contributed to this work.

https://doi.org/10.1016/j.jddst.2018.10.032
Received 20 August 2018; Received in revised form 8 October 2018; Accepted 26 October 2018
Available online 28 October 2018
1773-2247/

received much attention as promising and efficient colloidal carrier systems for the enhancement of dermal and transdermal delivery [13,14]. NLC as a delivery system for topical treatment provides several advantages such as high skin permeation, sustainable drug release due to solidified lipid matrix, and occlusive properties that increase skin hydration. The nano-sized structure and unique lipid composition ensure the close contact between the particle and the skin, thereby increasing the residence time of the particles in the skin and enhancing its transport through the skin layer. NLC is also reported to improve drug stability and provide high drug concentration in the targeted area [15–18]. All of these characteristics deem NLC as a suitable drug delivery system for the topical treatment of hyperpigmentation. In recent years, several NLCs such as *N*-acetyl glucosamine, hydroquinone, and deoxyarbutin-loaded NLCs have been reported for the treatment of hyperpigmentation [14,19,20]. In addition, NLCs as second-generation nanolipid carriers developed from solid lipid nanoparticles were shown to overcome the limitations of solid lipid nanoparticles, such as drug expulsion on storage, low drug loading, and high water content [21]. Thus, NLC is postulated to be an ideal carrier for MHY908 delivery, as evident from the high drug loading, stability, and efficient skin permeation to facilitate significant anti-melanogenesis activities of MHY908.

In this study, we developed MHY908-loaded NLCs (MHY908/NLCs) to enhance skin permeation of MHY908 for the treatment of hyperpigmentation. Physicochemical properties of MHY908/NLCs were evaluated and the *in vitro* drug release, occlusive property, and *ex vivo* skin permeation of MHY908/NLCs were investigated. The *in vitro* anti-melanogenesis activity of MHY908/NLCs was evaluated using a UVB-induced hyperpigmentation C57BL/6 mouse model. In addition, the *in vitro* cytotoxicity of MHY908/NLCs in L929 fibroblast cells was studied.

2. Materials and methods

2.1. Materials

MHY908 was synthesized as previously reported [22]. Compritol® 888 ATO comprising mono-, di-, and triesters of behenic acid [C22] was chosen as the solid constituent of NLC and received as a generous gift from Gattefossé (Saint-Priest, France). Miglyol®812, used as a liquid constituent of NLC, was purchased from CREMER OLEO KG (Hamburg, Germany). Phospholipon 90 G (phosphatidylcholine 90%) was a gift from Lipoid GmbH (Ludwigshafen, Germany) and used as a co-surfactant. The surfactant used was Poloxamer 188 (Pluronic®F68) purchased from Sigma-Aldrich (St Louis, MO, USA). Phosphotungstic acid, tetrazolium dye 3-(4,5-di-methylthiazol-2-yl)-2,5 diphenyltetrazolium bromide (MTT) reagent, and dimethyl sulfoxide (DMSO) were obtained from Sigma-Aldrich. Roswell Park Memorial Institute (RPMI)-1640 medium, trypsin, fetal bovine serum, and penicillin-streptomycin were procured from HyClone (Logan, UT, USA). All other reagents and solvents used were of the highest analytical grade.

2.2. Preparation of MHY908/NLCs

A reverse injection technique of melt and ultrasonication was slightly modified to fabricate MHY908/NLCs [23]. Briefly, the oil phase was prepared by melting the lipid mixture (Compritol/Miglyol 2:1) at 80 °C. A total of 5 mg of MHY908 was added to the molten lipid mixture and allowed to dissolve for a few minutes. The water phase comprising 1% Poloxamer 188 solution was heated to the same temperature and injected into the oil phase using an injector (Syringe pumps, KD Scientific, USA) at a rate of 4 mL/min. The resulting coarse mixture was emulsified using a homogenizer (IKA®T10 basic ULTRA- TURRAX®, Germany) at 15,000 rpm for 3 min. The emulsion was immediately ultra-sonicated (KFS-300 N Ultrasonic, Korea) at 270 W for 5 min, and the nano-dispersion was cooled down to 25 °C by mild stirring for 1 h. After cooling, the resultant NLCs were collected by centrifugation (LaboGene - 1736R, Korea) at 15,000 × *g* for 45 min at 4 °C and re-suspended in double distilled water for further application.

2.3. Characterization of MHY908/NLCs

2.3.1. Transmission electron microscopy (TEM) analysis

The morphological characteristics of MHY908/NLCs were observed using a TEM instrument (H-7600, Hitachi, Japan). Negative staining method was employed to prepare TEM samples to provide a contrast for the visualization of dried NLC specimens on a copper grid (200-mesh formvar copper grid). The samples were diluted for TEM observation.

2.3.2. Particles size and zeta potential measurement

The mean particle size, polydispersity index (PDI), and zeta potential were confirmed using a Zetasizer Nano series ZS90 (Malvern instruments Ltd, Worcestershire, UK). The average particle size and PDI of NLCs were determined by dynamic light scattering (DLS). All the measurements were performed at a fixed angle of 90° in Milli-Q water at 25 °C with three repetitions. For the zeta potential measurement, disposable folded capillary cell DTS 1070 was used. The particle size of NLC and the size distribution were described by the cumulants mean (z-average) diameter and PDI values, respectively.

2.3.3. Differential scanning calorimetry (DSC) analysis

We performed DSC analysis using DSC-8000 (PerkinElmer Inc, USA), and the kinetics were quantitatively analyzed by SmartScan software™ system provided by PerkinElmer®. For DSC measurement, 10 mg of powdered samples (bulk Compritol® 888 ATO, MHY908, physical mixture [Compritol 888:MHY908 = 70:30], blank NLC, and MHY908/NLCs) were put into a standard aluminum pan. Thermogram was recorded by heating the sample at a rate of 10 °C/min in the temperature range from 20 °C to 220 °C. Nitrogen as a flushing gas was used (purging rate, 20 mL/min) throughout the experiment.

2.3.4. X-ray diffraction (XRD) analysis

We performed XRD analysis using a D8 ADVANCE with Davinci (Bruker AXS Inc., GmbH, Germany). The samples to be tested (bulk Compritol® 888, MHY908, blank NLC, and MHY908/NLCs) were mounted on the XRD pan. For instrumentation, a panalytical XRD (PANalytical X'Pert3 X-ray) equipped with copper anode (Cu Kα radiation, λ = 0.15418 nm) was used to obtain diffractograms using vertical goniometer (theta-theta) as a detector. The scanning study was conducted at a temperature range of 24 °C–25 °C.

2.3.5. Drug loading and encapsulation efficiency

The concentration of MHY908 loaded in NLCs was determined using high-performance liquid chromatography (HPLC, Shimadzu, Tokyo, Japan) analysis. The HPLC system was equipped with LC-20AT liquid chromatograph, SPD-20A Prominence UV/Vis detector, CT-20A Prominence column oven, DGU-20ASR degassing unit and SIL-20 Prominent auto sampler. A Luna C18 column (150 mm × 4.6 mm, 5 µm; Phenomenex, USA) was used. The mobile phase used was a combination of phosphate-buffered saline (PBS; pH 8) and acetonitrile (60:40, v/v) and a volume of 40 µL was injected at a flow rate of 0.8 mL/min. For the assessment of MHY908, a calibration curve was obtained from a series of standard solutions of MHY908 in absolute ethanol at concentrations ranging from 0.03 to 250 µg/mL. The retention time for MHY908 was 5 min and the wavelength of maximum absorption was 218 nm.

The total amount of MHY908 loaded in NLC was determined by dissolving an appropriate amount of freeze-dried MHY908/NLC in absolute ethanol, followed by its analysis under chromatographic conditions mentioned above. Drug loading (%) and drug encapsulation efficiency (EE, %) were calculated using the following equations:

$$\text{Drug loading (\%)} = \frac{\text{MHY908 in NLCs (mg)}}{\text{Total NLCs weight (mg)}} \times 100$$

$$\text{EE (\%)} = \frac{\text{Amount of MHY908 in NLCs (mg)}}{\text{Amount of MHY908 initially added (mg)}} \times 100$$

2.4. In vitro drug release from MHY908/NLCs

The release of MHY908 from MHY908/NLCs was evaluated in 1% Tween-80/PBS (pH 7.4) at 37 °C using Visking tubing membrane-mediated dialysis method. The Visking membrane was immersed in a fresh buffer solution overnight prior to the *in vitro* release study and filled with an appropriate amount of MHY908/NLC suspension (equivalent to 2 mg of MHY908) in 200 mL of buffer solution, followed by its incubation in a shaking water bath (37 °C) at 100 rpm. At predetermined time intervals, an aliquot (1 mL) of the medium was withdrawn and volumes were made up with fresh buffer solution. One-hundred microliters of supernatant was withdrawn. The released MHY908 was quantified using HPLC as described above. All the measurements were performed in triplicates.

2.5. In vitro and ex vivo occlusion test

In vitro occlusion property of MHY908/NLCs was evaluated using a modified method, as previously reported [24]. In brief, 100-mL beakers were filled with 50 mL of distilled water and covered with filter paper (cellulose acetate membrane filter, 90 mm, Sterlitech, USA); filter papers were attached to beakers using parafilm. MHY908/NLCs (200 mg) were applied onto the filter paper and evenly spread, leading to a physical film formation at the surface. The whole experiment was conducted in a controlled environment (temperature, 32 °C; relative humidity, 50%–55%) for 48 h. Beakers were weighed at specific time intervals (6, 12, 24, and 48 h).

Ex vivo occlusion experiment was performed with a slight modification from a reported method [25]. Male Wistar rats (Wistar Hannover 170–220 g, Samtako Bio, Korea) were selected for *ex vivo* study. Rat abdominal skin was processed and collected according to the procedure described above. Ice-cooled normal saline was used to maintain the integrity of the surgically removed skin and the samples were stored at −20 °C before use. Glass beakers (100 mL) were filled with distilled water (50 mL), clenched carefully with the rehydrated skin specimen, and placed into a close-fitting plastic container. The occlusivity (*in vitro* and *ex vivo*) was calculated with the following equation:

$$F = \frac{A - B}{A} \times 100$$

Where, F is the occlusion factor, A is the water loss from the reference beaker, and B is the water loss from the sample beaker.

2.6. Ex vivo skin permeation study

Ex vivo skin permeation studies of MHY908 solution and MHY908/NLCs were carried out for 48 h at 32 °C by a static diffusion cell system (Franz™ diffusion cell) using skin of C57BL/6 mice (mean thickness of 242.70 ± 39.83 μm) as the diffusion membrane. Briefly, the skin was collected and the adhering subcutaneous fatty tissues were carefully removed using blunt tweezers. The samples were subsequently immersed in cold normal saline (pH 7.4). The skin specimens were pre-equilibrated with the receptor medium for 1 h before mounting on Franz™ diffusion cell. The receptor compartment (7 mL) consisted of a mixture of PBS (pH 7.4) and absolute ethanol (85:15 v/v) stirred at 100 rpm. A mixture of PBS (pH 7.4) and absolute ethanol (85:15 v/v) was used as the receptor medium to maintain the sink condition. An appropriate amount of each sample (containing 0.3 mg of MHY908) was incubated in the donor compartment and a 1-mL aliquot was withdrawn from the receptor compartment at predetermined time intervals and replaced with an equal volume of fresh medium (32 °C). All sampled aliquots were filtered through the hydrophilic syringe filter (pore size of 0.2 μm, Minisart NML, Germany) and analyzed by HPLC as described above. The experiment was repeated thrice and the results were expressed as mean ± standard deviation (SD).

The cumulative amount of MHY908 permeated (Q) per unit area of the mouse skin (μg/cm^2) was calculated and plotted against time. The steady-state skin flux (J_{SS}), lag time (t_{lag}), and permeability coefficient (K_P) of the drug were determined from the slope of a linear portion of the plot and calculated with the following equation [26]:

$$K_P = J_{SS}\, C_V^{-1}$$

Where J_{SS} is the steady-state flux through the skin and C_V is the initial concentration of MHY908 in the donor compartment. The enhancement factor (F_E) was determined using the following equation [27]:

$$F_E = \frac{Q_{NLC}}{Q_{Solution}}$$

Where Q_{NLC} is the cumulative amount of MHY908 permeated from NLC and $Q_{Solution}$ is the cumulative amount of MHY908 permeated from the solution.

2.7. In vivo anti-melanogenesis activity

The *in vivo* anti-melanogenesis activity of MHY908/NLCs was conducted in accordance with the regulation of Pusan National University and Korean Legislation on animal studies. Male C57BL/6 mice (5 weeks, Samtako Bio Korea) were used as animal models. The mice dorsal skin hair was trimmed off using an electric trimmer and hair removal cream. Mice were randomly divided into four experimental groups (6 mice/group) as follows: control group (UVB-radiated), MHY908 solution group (150 μg/mL), blank NLC group, and MHY908/NLC group (150 μg/mL). To induce pigmentation, each group was exposed to UVB radiation (λ = 312 nm) at an intensity of 150 mJ/cm^2 for 5 min using an Ultraviolet Crosslinkers (CL-1000 Ultraviolet Crosslinker, CA, USA). UVB radiation treatment was performed on every alternate day for 2 weeks. MHY908/NLC suspension and MHY908 solution were applied to a designated site (2 cm × 2 cm) on the mice skin every 2 days for 2 weeks. Skin-lightening index was measured using a CR-10 spectrophotometer (Konica Minolta Sensing, Sakai, Osaka, Japan) and presented as L*, a*, and b* as per the Commission Internationale de l'Eclairage color system.

2.8. In vitro cytotoxicity study

L929 mouse fibroblast cells (KCLB, Seoul, South Korea) were grown in RPMI-1640 culture medium. The culture medium was supplemented with 10% (v/v) fetal bovine serum, 100 IU/mL penicillin G sodium, and 100 μg/mL streptomycin sulfates. The cells were overnight incubated in a humidified atmosphere with 5% CO_2 (37 °C). Cells were seeded at a density of 5 × 10^4 cells/well in 96-well plates and incubated for 24 h. Upon reaching confluency, the medium containing floating cells was removed and fresh medium containing blank NLCs and MHY90/NLCs at varying concentrations (75, 150, 300, and 600 μg/mL) was added. The cells were incubated for another 24 h. A standard MTT solution in sterile PBS was added to each well and incubated for 2 h. Following incubation, MTT solution was replaced with 150 μL of DMSO. The absorbance measured at 540 nm wavelength was proportional to the number of viable cells in each well. Untreated cells were used as a control. The data were expressed as mean ± SD of eight replicates (n = 8). The cell viability was calculated using the following equation:

$$\text{Cell viability (\%)} = \frac{\text{Absorbance (treated cells)}}{\text{Absorbance (control cells)}} \times 100$$

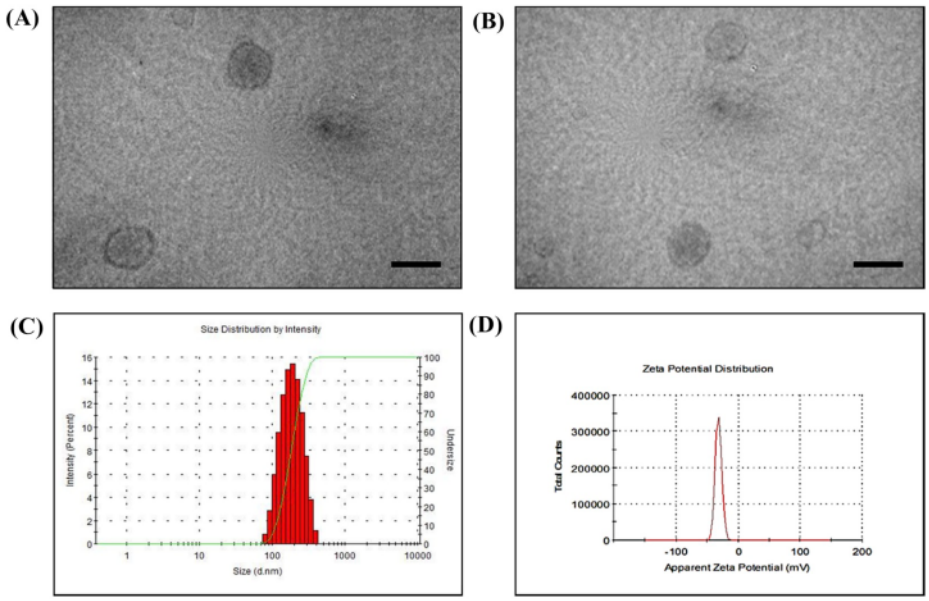

Fig. 1. Characterization of NLCs. (A) and (B) TEM image of blank NLCs and MHY908/NLCs, respectively. Bars represent 200 nm. (C) Size and (D) zeta potential distribution of MHY908/NLCs measured by Zetasizer Nano series ZS90.

2.9. Statistical analysis

Statistical analysis of *in vivo* data was performed using two-way analysis of variance (ANOVA), followed by Bonferroni test in GraphPad Prism 5.0 (GraphPad Software, Inc., LA Jolla, CA, USA). A value of $P < 0.05$ was considered statistically significant.

3. Results

3.1. Preparation and characterization of MHY908/NLCs

Nanoparticles (MHY908/NLC and blank NLC) used in this study were prepared by reverse injection technique of melt and ultrasonication. TEM images for the prepared NLCs revealed their spherical morphology (Fig. 1A and B). The average size of the blank NLC and MHY908/NLC was 198 ± 6 nm and 193 ± 2.4 nm, respectively (Table 1 and Fig. 1C). The PDI value of blank NLC (0.2) and MHY908/NLC (0.3) showed that the particles exhibit moderate polydisperse distribution (Table 1). Zeta potential measurements (Table 1 and Fig. 1D) revealed that both blank NLCs and MHY908/NLCs were negatively charged (−31 ± 0.6 and −32 ± 1.2 mV, respectively). Fig. 2A shows the DSC curves of the melting process of Compritol 888 ATO, MHY908, physical mixture (solid lipid + drug), blank NLCs, and MHY908/NLCs. The physical mixture showed a distinctive peak of MHY908 at around 203 °C. For MHY908/NLCs, however, the characteristic peak of MHY908 disappeared. In addition, both blank NLCs and MHY908/NLCs demonstrated identical peaks from 55 °C to 75 °C. Both NLCs showed same peaks as Compritol® 880 ATO at 73 °C; the difference was the presence of a peak at 55 °C for NLCs, which indicated

Table 1
Physicochemical properties of MHY908/NLCs.

NLCs	Drug loading (%)	EE (%)	Size (nm)	PDI	Zeta potential (mV)
Blank NLC	NA	NA	193 ± 2.4	0.2 ± 0.04	−31 ± 0.6
MHY908/NLCs	4 ± 0.02	89 ± 1.4	198 ± 6	0.3 ± 0.2	−32 ± 1.2

Values are expressed as mean ± S.D. (n = 3).

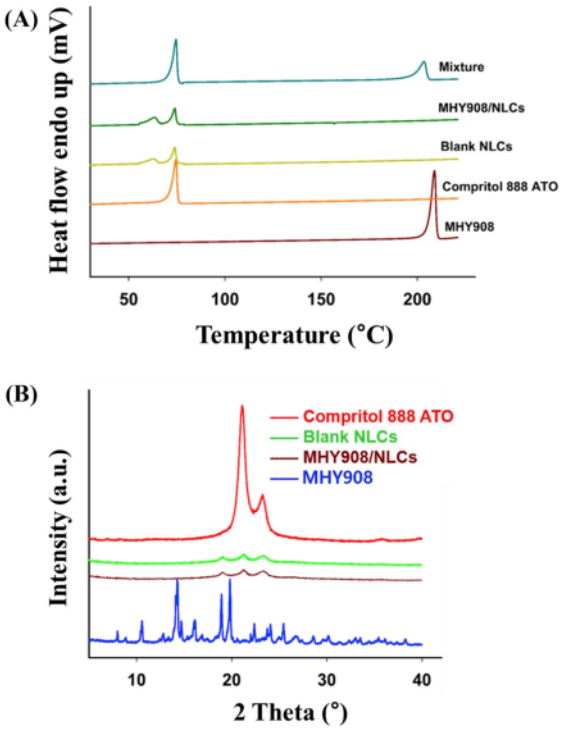

Fig. 2. DSC and XRD analyses. (A) DSC scans of mixture, MHY908/NLCs, blank NLCs, Compritol 888 ATO, and MHY908. (B) XRD of MHY908/NLCs, blank NLCs, Compritol 888 ATO, and MHY908.

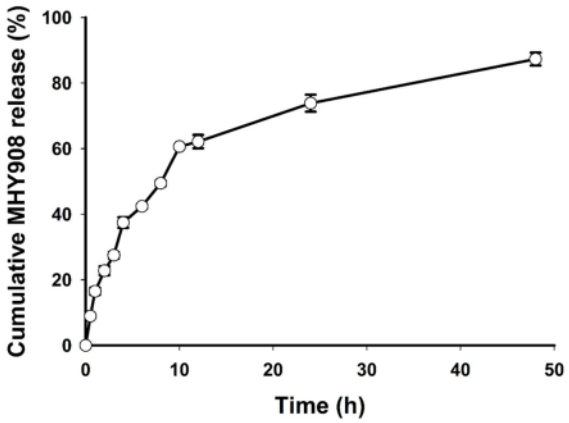

Fig. 3. *In vitro* release profile of MHY908/NLCs. All samples were placed in PBS (pH 7.4) and ethanol mixture. Values are expressed as mean ± SD (n = 3).

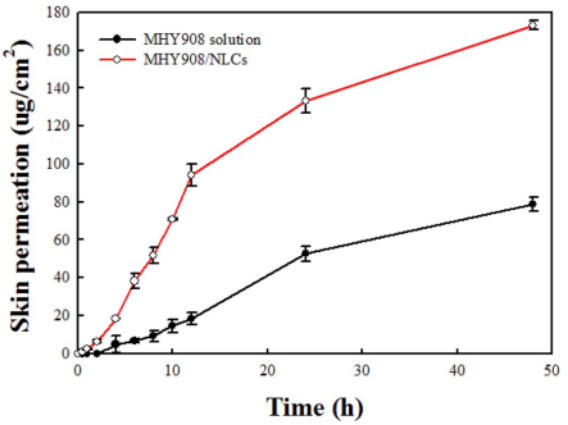

Fig. 5. *In vitro* skin permeation profile of MHY908 solution and MHY908/NLCs. Values are expressed as mean ± SD (n = 3).

liquid lipid (Miglyol® 812). The bulk MHY908 showed an endothermic melting peak at around 208 °C. Moreover, the melting point of Compritol® 888 ATO slightly decreased in MHY908/NLCs from 74 °C to 73 °C. The XRD patterns of Compritol® 888 ATO, MHY908, blank NLCs, and MHY908/NLCs are displayed in Fig. 2B. The XRD data were in line with the results of DSC measurement, wherein the MHY908 exhibited a crystal form, while the diffraction pattern of MHY908/NLCs revealed the amorphous state. In addition, Compritol® 888 ATO had a diffraction peak at 2θ of 21.23° and 23.30° corresponding to the short spacing at 0.42 and 0.38 nm respectively. However, the intensities of two characteristic peaks reduced in MHY908/NLCs.

The profile of MHY908 release from MHY908/NLCs is shown in Fig. 3. MHY908 showed a biphasic release pattern, with an initial burst release followed by prolonged and sustained release for over 2 days. MHY908/NLCs exhibited burst release of MHY908 (~60%) in the first 10 h and ~87% released thereafter in 48 h.

3.2. Occlusive property of MHY908/NLCs

In vitro and *ex vivo* occlusive properties of MHY908/NLCs are shown in Fig. 4. MHY908/NLCs showed significantly higher occlusivity than MHY908 solution *in vitro* after 48 h (Fig. 4 left y-axis). A gradual increase in occlusion was observed for MHY908/NLCs for up to 48 h. However, a gradual decrease in the occlusion factor was observed in *ex vivo* samples (Fig. 4 right y-axis), wherein the skin was used as the barrier for occlusion study. The *ex vivo* occlusion results are in agreement with the *in vitro* study, wherein MHY908/NLCs showed significantly higher occlusion effect than MHY908 solution.

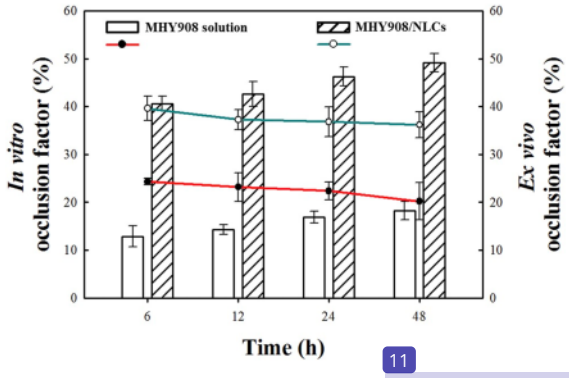

Fig. 4. *In vitro* and *ex vivo* occlusion study. Values are expressed as mean ± SD (n = 3).

3.3. Ex vivo skin permeation study

Ex vivo skin permeation study of MHY908 solution and MHY908/NLCs was conducted using static diffusion cell system (Franz™ diffusion cell) and the results are shown in Fig. 5. MHY908/NLCs showed two-fold higher skin permeation than MHY908 solution. Approximately 57.7% of MHY908 permeated from MHY908/NLCs through the skin after 48 h. On the contrary, only 26.3% of MHY908 in the solution showed skin permeation. Table 2 describes the *ex vivo* skin permeation parameters such as lag time (t_{lag}), steady-state skin flux (J_{ss}), permeability coefficient (K_p), and enhancement factor (F_E). MHY908/NLCs showed rapid penetration through the skin, as evident from the shorter lag time (t_{lag} = 0.5 h) than MHY908 solution (t_{lag} = 2 h). In addition, MHY908/NLCs showed higher flux (3.6 ± 0.05 μg cm^{-2} h^{-1}) than MHY908 solution (1.6 ± 0.07 μg cm^{-2} h^{-1}). The value of the coefficient of permeability (K_P) for MHY908/NLCs (120.3 ± 1.8 × 10^{-4} cm/h) was in line with the flux result and higher than that of MHY908 solution (54.7 ± 2.4 × 10^{-4} cm/h).

3.4. In vivo anti-melanogenesis activity

The qualitative and quantitative skin-lightening effect of UVB-induced hyperpigmentation in mice treated with MHY908 solution, blank NLCs, or MHY908/NLCs are presented in Fig. 6. Fig. 6A shows the results of skin-lightening effect (qualitative) and the protective effect of MHY908/NLCs after topical application for 14 days. Visual assessment revealed the significant increase in the skin lightness for mice treated with MHY908/NLCs than those treated with UV, MHY908 solution, and blank NLCs for up to 14 days. While the UV control and blank NLC group showed no protective effect against UVB exposure, mice treated with MHY908 solution showed skin-lightening effect; however, the effect was not as high as that observed with MHY908/NLC treatment. The result was in line with the quantitative skin-lightening effect determined using CR-10 spectrophotometer (Fig. 6B). The L-value (skin-luminosity index), known as the degree of pigmentation, ranging from L = 100 (white; 64–68 denote bright skin) to L = 0 (black; 40–45 denote dark skin) is the total quantity of light reflected by the skin and describes the skin-lightening index. Before UVB radiation and treatment initiation, the L-value for all groups was between 64.0 and 66.8 and was considered relatively bright. The L-value of all UVB-treated groups gradually decreased upon UVB exposure. The topical application of the tested formulations for 14 days resulted in the reduction in hyperpigmentation, with MHY908/NLC

Table 2
In vitro skin permeation parameters.

Formulations	J_{ss} (μg.cm^{-2}.h^{-1})	$K_P \times 10^{-4}$ (cm h^{-1})	t_{lag} (h)	F_E
MHY908 solution	1.6 ± 0.07	54.7 ± 2.4 × 10^{-4}	2	NA
MHY908/NLCs	3.6 ± 0.05	120.3 ± 1.8 × 10^{-4}	0.5	2.2 ± 0.07

Values are expressed as mean ± S.D. (n = 3).

treatment (L = 61.4) being the most effective in the prevention of the gradual decrease in L values. Therefore, a significant depigmentation effect was observed with MHY908/NLC as compared to others, owing to the combined effects of permeation enhancement and large surface area. The lightening effect observed with MHY908 solution (L = 50.4) was lower than that observed with MHY908/NLCs after 14 days. In contrast, blank NLCs showed almost no anti-melanogenic activity (L = 40.2) after 14 days of treatment.

3.5. *In vitro* cytotoxicity study

Cytotoxicity of blank NLCs and MHY908/NLCs are shown in Fig. 7. Both blank NLCs and MHY908/NLCs revealed no significant cytotoxicities (> 80% viability) in L929 fibroblast cells at concentrations up to 600 μg/mL. However, the percentage of viable cells remained higher than 85% for groups treated with MHY908/NLCs at concentrations lower than 600 μg/mL.

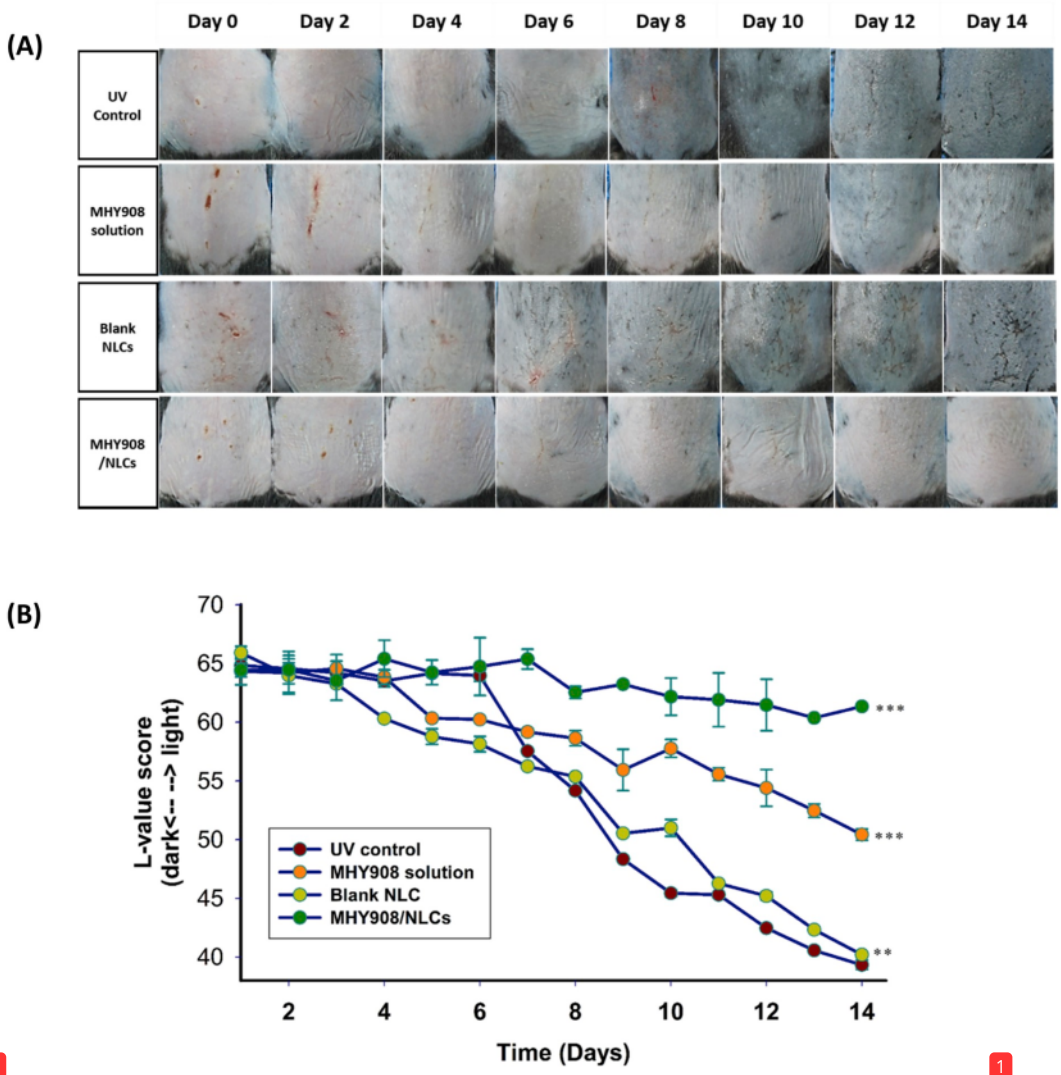

Fig. 6. *In vivo* evaluation of depigmentation activity. (A) Qualitative skin brightness results of UVB-induced melanogenesis. (B) Quantitative skin brightness was determined using a CR-10 spectrophotometer. Values are expressed as mean ± SD (n = 3). ***$P < 0.001$ for MHY908/NLC and MHY908 solution groups, and **$P < 0.05$ for blank NLC group when compared with the UV-treated control group.

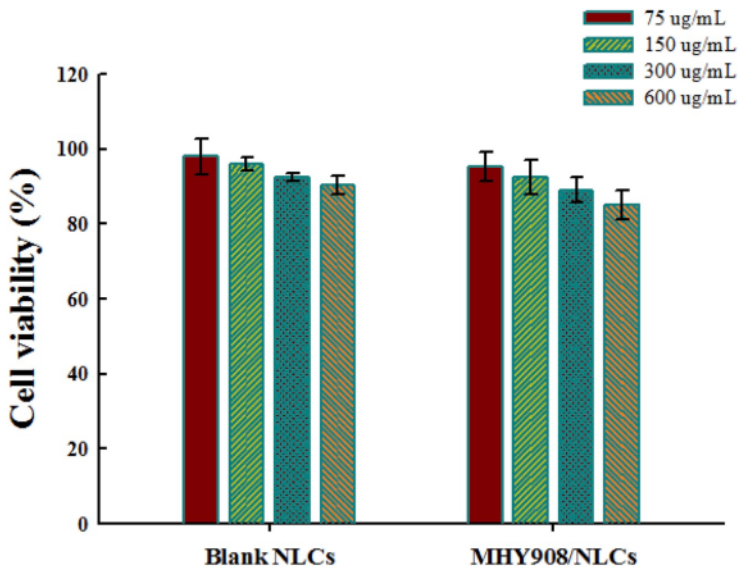

Fig. 7. ***In vitro*** **cytotoxicity study.** The cytotoxicity study was conducted on L929 cell line. Values are expressed as mean ± SD (n = 3).

4. Discussion

The aim of this study was to develop MHY908-loaded NLCs that efficiently deliver MHY908 to basal layer of epidermis (melanocyte cell) for the treatment of hyperpigmentation. Reverse injection technique of melt and ultrasonication was employed as an improved version to produce NLCs [23]. The drawbacks of a regular melt and ultrasonication method (direct method) include drug loss and formation of lipid aggregates that float in NLC suspension, owing to the adhesion phenomenon of the remaining molten lipids in the glassware during its addition to water [28]. To address this problem, the reverse injection technique was developed. In this method, in contrast to the previous method, the water phase is inserted into the oil phase to prevent the formation of lipid aggregation and reduce drug loss. This modified technique resulted in MHY908/NLCs with sufficient drug loading (4%) and high EE (> 80%) (Table 1). Particle size characterization revealed that there is no size difference for MHY908/NLCs and blank NLC, indicating that the presence of MHY908 had no effect on NLC size. Both NLCs showed a value higher than − 30 mV, indicating that the prepared NLCs possess higher colloidal system stability during storage. The high zeta potential value prevents particle aggregation owing to the electrostatic repulsion amongst particles, indicative of their good physical storage stability [29].

We performed DSC and XRD analyses to evaluate physicochemical characterization of MHY908/NLCs in term of melting and recrystallization behavior and also polymorphic behavior. The DSC analysis results revealed that the physical mixture showed a distinctive peak of MHY908, indicating that MHY908 fails to completely dissolve in Compritol® 888 ATO. For MHY908/NLCs, however, the characteristic peak of MHY908 disappeared, demonstrating the incorporation of MHY908 in NLC matrix in an amorphous state (Fig. 2A). The XRD data were in line with the results of DSC measurement, wherein the diffraction pattern of MHY908 revealed a notable difference from that of MHY908/NLCs (Fig. 2B). MHY908 exhibited a crystal form, while the diffraction pattern of MHY908/NLCs revealed the amorphous state. In addition, Compritol® 888 ATO had a diffraction peak at 2θ of 21.23° and 23.30° corresponding to the short spacing at 0.42 and 0.38 nm respectively, indicative of its polymorphic β′ form [30]. The polymorphism of Compritol® 888 ATO was associated with the distinct hydrocarbon chain arrangement in behenic acid that exhibited crystallinity in α and β′ or α, β, and β′ episodes [31]. However, the intensities of two characteristic peaks reduced in MHY908/NLCs, suggesting that MHY908 was molecularly dispersed within the crystal lattice of the lipid blend of Compritol® 888 ATO and Miglyol® 812. It was clear that the amorphous state or less ordered crystals of MHY908/NLCs were related to the disappearance of the sharp peak of the pure drug (MHY908) [32]. This observation revealed the loading of MHY908 into NLCs and indicated the high entrapment and loading efficiency.

The *in vitro* release study was performed to assess MHY908 release behavior from the NLC matrix. As shown in Fig. 3, MHY908 showed a biphasic release pattern. Initial rapid drug diffusion may be advantageous for topical formulations, wherein higher concentration gradient of drugs is always expected owing to the enhanced skin penetration effect [21]. The slow release rate of MHY908 from MH908/NLCs revealed the linear relationship with Higuchi release kinetic model (R^2 = 0.9838) over 48 h that showed drug diffusion from the matrix. This prolonged release pattern of drugs may be explained by the enrichment of MHY908 in the lipid matrix of NLCs, followed by a slow diffusion that allowed sustained release [33]. The release behavior of MHY908 demonstrated that the dual release kinetics could play an important role for MHY908/NLC as a drug delivery system to skin. The initial burst release provides a favorable concentration gradient for skin permeation, while the sustained release maintains MHY908 concentration in the targeted area, leading to a prolonged anti-melanogenesis effect.

The occlusive property of MHY908/NLCs was investigated because NLCs can form a continuous thin film on the skin, followed by skin hydration by inhibiting transepidermal water loss (TEWL), resulting in enhanced penetration of drugs across the stratum corneum. The consequence of this effect is wide inter-corneocyte gaps and enhanced drug penetration [34]. As shown in Fig. 4 (left y-axis), MHY908/NLCs showed significantly higher occlusivity than MHY908 solution *in vitro* after 48 h. This may be associated with the effective blocking of filter pores by lipid particles, while the solution lacked the ability to provide occlusion. A gradual increase in occlusion was observed for MHY908/NLCs for up to 48 h, might be due to the gradual pack formation by lipid nanoparticles, resulting in a continuous progress in the block formation. Different from the *in vitro* study, the skin continuously destabilized the

lipid film by interacting with biodegradable lipids of NLCs in *ex vivo* study. This could possibly allow some water evaporation, leading to a gradual decrease in the occlusivity with time. In both study settings, MHY908/NLCs were able to maintain a suitable occlusivity, highlighting the potentiality of MHY908/NLCs for high skin penetration.

Ex vivo skin permeation results showed that MHY908/NLCs has higher permeation than MHY908 solution (Fig. 5), may be attributed to the large surface area of the particles that interacted with corneocytes of the stratum corneum as well as the increased hydration effect of the occlusive property, as previously discussed. In addition, Poloxamer 188 used as a surfactant in NLCs contributed to the improved permeation by fluidizing lipid bilayers of the stratum corneum [35]. MHY908/NLCs showed rapid penetration through the skin, more evident from the shorter lag time than MHY908 solution that suggests faster permeation initiation to reach steady-state. In addition, MHY908/NLCs showed higher flux and coefficient of permeability (K_P) than MHY908 solution. Thus, these results confirmed that the enhanced permeability of MHY908/NLCs resulted from the film-forming ability of NLCs, which is absent in MHY908 solution. The film formation facilitates skin hydration through the inhibition of TEWL. This phenomenon led to the swelling of the tight arrangement of the stratum corneum and loosening of the corneocyte packing, thereby enhancing the permeation of MHY908 through the skin.

The *in vivo* anti-melanogenesis activity of MHY908/NLCs was evaluated by inducing UVB-mediated hyperpigmentation in C57BL/6 mouse. The underlying mechanism of UVB-induced melanogenesis is the upregulation in the expression of tyrosinase gene, the rate-limiting gene in melanin synthesis, and the increase in alpha melanocyte-stimulating hormone receptor activity through direct effects of UV photons on DNA molecules [36]. Thus, these factors stimulate melanocyte mitosis, increase melanin production, and enhance the movement of melanin throughout the skin surface. Such cascades are responsible for hyperpigmentation and skin darkening. As shown in Fig. 6, MHY908/NLCs effectively prevented UVB-induced hyperpigmentation than MHY908 solution. The higher efficiency of MHY908/NLC formulations may be attributed to the high concentration of MHY908 in melanocytes through the occlusive effect of lipids provided by NLCs, leading to efficient skin permeation. In general, the intercellular pathway in the lipid bilayer is the primary permeation route for most lipophilic agents to pass through the stratum corneum barrier. Destabilization of the lipid barrier through the prevention of TEWL may possibly enhance the permeation of lipophilic compounds such as MHY908. Moreover, NLC formulation proved to be an excellent delivery system for the percutaneous absorption of lipophilic agents through the stratum corneum because of the large surface area of the nano-sized particles. Therefore, a significant depigmentation effect was observed with MHY908/NLC as compared to others, owing to the combined effects of permeation enhancement and large surface area. The lightening effect observed with MHY908 solution was lower than that observed with MHY908/NLCs after 14 days. This observation may be possibly related to the penetration effect of propylene glycol and ethanol in the skin; however, this effect had no significant influence on the prevention of hyperpigmentation. In contrast, blank NLCs showed almost no anti-melanogenic activity after 14 days of treatment, indicative of the absence of any role in the prevention of melanin overproduction. The above evaluation of the anti-melanogenesis activity based on the qualitative and quantitative analyses demonstrated the higher efficacy of MHY908/NLCs in melanin inhibition.

Cytotoxicities of blank NLCs and MHY908/NLCs were evaluated in the mouse fibroblast cell line, L929, a commonly used model cell line for evaluating the biocompatibility of topically applied formulations [37]. As shown in Fig. 7, the released MHY908 from MHY908/NLCs has no damaging effects on healthy fibroblasts. Moreover, the particle concentration used for the *in vivo* anti-melanogenesis activity analysis was only 150 μg/mL. Moreover, the lipid blend of NLC is considered safe and bio-compatible.

5. Conclusions

MHY908-loaded nanostructured lipid carriers (MHY908/NLCs) have been successfully fabricated with sufficient drug loading. DSC and XRD analyses revealed that MHY908, which per se exhibits a crystal state, becomes an amorphous state when encapsulated in the NLCs. MHY908/NLCs exhibited a dual drug release kinetic (initial burst release followed by prolonged drug release) and higher skin permeation than MHY908 solution. In *in vitro* and *ex vivo* occlusion studies, MHY908/NLCs showed significantly higher occlusion effect than MHY908 solution. Furthermore, MHY908/NLCs effectively prevented UVB-induced hyperpigmentation and showed no toxicity to skin fibroblast cells. Thus, MHY908/NLCs investigated in this study could serve as a promising topical delivery system for the treatment of hyperpigmentation.

Conflicts of interest

The authors report no conflicts of interest. The authors alone are responsible for the content and writing of this article.

Acknowledgement

This work was supported by a 2-year Research Grant of Pusan National University.

References

[1] G. Prota, Melanins and Melanogenesis, Academic Press, 2012.
[2] A. Kawakami, D.E. Fisher, Key discoveries in melanocyte development, J. Invest. Dermatol. 131 (2011) E2–E4.
[3] R.M. Halder, P.K. Nootheti, Ethnic skin disorders overview, J. Am. Acad. Dermatol. 48 (2003) S143–S148.
[4] N. Chen, Y. Hu, W.H. Li, M. Eisinger, M. Seiberg, C.B. Lin, The role of keratinocyte growth factor in melanogenesis: a possible mechanism for the initiation of solar lentigines, Exp. Dermatol. 19 (2010) 865–872.
[5] A. Stratigos, A. Forsea, R. Van Der Leest, E. De Vries, E. Nagore, J.L. Bulliard, M. Trakatelli, J. Paoli, K. Peris, J. Hercogova, Euromelanoma: a dermatology-led European campaign against nonmelanoma skin cancer and cutaneous melanoma. Past, present and future, Br. J. Dermatol. 167 (2012) 99–104.
[6] J.P. Ebanks, R.R. Wickett, R.E. Boissy, Mechanisms regulating skin pigmentation: the rise and fall of complexion coloration, Int. J. Mol. Sci. 10 (2009) 4066–4087.
[7] A. Slominski, D.J. Tobin, S. Shibahara, J. Wortsman, Melanin pigmentation in mammalian skin and its hormonal regulation, Physiol. Rev. 84 (2004) 1155–1228.
[8] S. Parvez, M. Kang, H.S. Chung, C. Cho, M.C. Hong, M.K. Shin, H. Bae, Survey and mechanism of skin depigmenting and lightening agents, Phytother Res. 20 (2006) 921–934.
[9] H. Ando, H. Kondoh, M. Ichihashi, V.J. Hearing, Approaches to identify inhibitors of melanin biosynthesis via the quality control of tyrosinase, J. Invest. Dermatol. 127 (2007) 751–761.
[10] M.H. Park, S.J. Kim, H.O. Jeong, K.M. Moon, S. Son, D.H. Kim, H.R. Kim, M.J. Kim, H.Y. Yun, P. Chun, Inhibition of melanogenesis by 2-[4-(5-chlorobenzo [d] thiazol-2-yl) phenoxy]-2-methylpropanoic acid (MHY908), Arch Pharm. Res. (Seoul) 38 (2015) 505–511.
[11] R. Marks, The stratum corneum barrier: the final frontier, J. Nutr. 134 (2004) 2017S–2021S.
[12] W.-s. Sung, S.-y. Oh, Electroosmotic flow through skin: effect of current duration and poly (ethylene imine), Journal of Pharmaceutical Investigation (2017) 1–7.
[13] S. Ghanbarzadeh, R. Hariri, M. Kouhsoltani, J. Shokri, Y. Javadzadeh, H. Hamishehkar, Enhanced stability and dermal delivery of hydroquinone using solid lipid nanoparticles, Colloids Surfaces B Biointerfaces 136 (2015) 1004–1010.
[14] L. Aliasgharlou, S. Ghanbarzadeh, H. Azimi, M.H. Zarrintan, H. Hamishehkar, Nanostructured lipid Carrier for topical application of N-acetyl glucosamine, Adv. Pharmaceut. Bull. 6 (2016) 581.
[15] E.H. Gokce, E. Korkmaz, E. Dellera, G. Sandri, M.C. Bonferoni, O. Ozer, Resveratrol-loaded solid lipid nanoparticles versus nanostructured lipid carriers: evaluation of antioxidant potential for dermal applications, Int. J. Nanomed. 7 (2012) 1841.
[16] M. Schäfer-Korting, W. Mehnert, H.-C. Korting, Lipid nanoparticles for improved topical application of drugs for skin diseases, Adv. Drug Deliv. Rev. 59 (2007) 427–443.
[17] R. Müller, R. Petersen, A. Hommoss, J. Pardeike, Nanostructured lipid carriers (NLC) in cosmetic dermal products, Adv. Drug Deliv. Rev. 59 (2007) 522–530.
[18] J. Pardeike, A. Hommoss, R.H. Müller, Lipid nanoparticles (SLN, NLC) in cosmetic and pharmaceutical dermal products, Int. J. Pharm. (Amst.) 366 (2009) 170–184.
[19] P.-S. Wu, C.-H. Lin, Y.-C. Kuo, C.-C. Lin, Formulation and characterization of hydroquinone nanostructured lipid carriers by homogenization emulsification method, J. Nanomater. (2017) 2017.

[20] R.P. Tofani, Y.C. Sumirtapura, S.T. Darijanto, Formulation, characterisation, and in vitro skin diffusion of nanostructured lipid carriers for deoxyarbutin compared to a nanoemulsion and conventional cream, Sci. Pharm. 84 (2016) 634–645.
[21] R.H. Müller, M. Radtke, S.A. Wissing, Solid lipid nanoparticles (SLN) and nanostructured lipid carriers (NLC) in cosmetic and dermatological preparations, Adv. Drug Deliv. Rev. 54 (2002) S131–S155.
[22] M.H. Park, J.Y. Park, H.J. Lee, D.H. Kim, D. Park, H.O. Jeong, C.H. Park, P. Chun, H.R. Moon, H.Y. Chung, Potent anti-diabetic effects of MHY908, a newly synthesized PPAR α/γ dual agonist in db/db mice, PloS One 8 (2013) e78815.
[23] E. Esposito, L. Ravani, M. Drechsler, P. Mariani, C. Contado, J. Ruokolainen, P. Ratano, P. Campolongo, V. Trezza, C. Nastruzzi, Cannabinoid antagonist in nanostructured lipid carriers (NLCs): design, characterization and in vivo study, Mater. Sci. Eng. C 48 (2015) 328–336.
[24] S. Wissing, A. Lippacher, R. Müller, Investigations on the occlusive properties of solid lipid nanoparticles (SLN), J. Cosmet. Sci. 52 (2001) 313–324.
[25] H. Hamishehkar, S. Same, K. Adibkia, K. Zarza, J. Shokri, M. Taghaee, M. Kouhsoltani, A comparative histological study on the skin occlusion performance of a cream made of solid lipid nanoparticles and Vaseline, Research in pharmaceutical sciences 10 (2015) 378.
[26] R.R. Gupta, S.K. Jain, M. Varshney, AOT water-in-oil microemulsions as a penetration enhancer in transdermal drug delivery of 5-fluorouracil, Colloids Surfaces B Biointerfaces 41 (2005) 25–32.
[27] M.M. Al-Subaie, K.M. Hosny, K.M. El-Say, T.A. Ahmed, B.M. Aljaeid, Utilization of nanotechnology to enhance percutaneous absorption of acyclovir in the treatment of herpes simplex viral infections, Int. J. Nanomed. 10 (2015) 3973.
[28] E. Esposito, M. Drechsler, R. Cortesi, C. Nastruzzi, Encapsulation of cannabinoid drugs in nanostructured lipid carriers, Eur. J. Pharm. Biopharm. 102 (2016) 87–91.
[29] V. Teeranachaideekul, E.B. Souto, V.B. Junyaprasert, R.H. Müller, Cetyl palmitate-based NLC for topical delivery of Coenzyme Q10–Development, physicochemical characterization and in vitro release studies, Eur. J. Pharm. Biopharm. 67 (2007) 141–148.
[30] V. Teeranachaideekul, E.B. Souto, V.B. Junyaprasert, R.H. Müller, Cetyl palmitate-based NLC for topical delivery of Coenzyme Q 10–Development, physicochemical characterization and in vitro release studies, Eur. J. Pharm. Biopharm. 67 (2007) 141–148.
[31] E. Souto, W. Mehnert, R. Müller, Polymorphic behaviour of Compritol® 888 ATO as bulk lipid and as SLN and NLC, J. Microencapsul. 23 (2006) 417–433.
[32] X. Liu, X. Feng, R.O. Williams, F. Zhang, Characterization of amorphous solid dispersions, Journal of Pharmaceutical Investigation (2017) 1–23.
[33] E.S. Farboud, S.A. Nasrollahi, Z. Tabbakhi, Novel formulation and evaluation of a Q10-loaded solid lipid nanoparticle cream: in vitro and in vivo studies, Int. J. Nanomed. 6 (2011) 611.
[34] R.H. Müller, U. Alexiev, P. Sinambela, C.M. Keck, Nanostructured lipid carriers (NLC): the second generation of solid lipid nanoparticles, Percutaneous Penetration Enhancers Chemical Methods in Penetration Enhancement, Springer, 2016, pp. 161–185.
[35] S.-C. Shin, C.-W. Cho, I.-J. Oh, Effects of non-ionic surfactants as permeation enhancers towards piroxicam from the poloxamer gel through rat skins, Int. J. Pharm. (Amst.) 222 (2001) 199–203.
[36] B.A. Gilchrest, H.Y. Park, M.S. Eller, M. Yaar, Mechanisms of ultraviolet light–induced pigmentation, Photochem. Photobiol. 63 (1996) 1–10.
[37] H. Nurhasni, J. Cao, M. Choi, I. Kim, B.L. Lee, Y. Jung, J.-W. Yoo, Nitric oxide-releasing poly (lactic-co-glycolic acid)-polyethylenimine nanoparticles for prolonged nitric oxide release, antibacterial efficacy, and in vivo wound healing activity, Int. J. Nanomed. 10 (2015) 3065.

11th Paper_Nurhasni Hasan (2018).pdf

ORIGINALITY REPORT

14%	12%	13%	3%
SIMILARITY INDEX	INTERNET SOURCES	PUBLICATIONS	STUDENT PAPERS

PRIMARY SOURCES

1	topsecretapiaccess.dovepress.com Internet Source	4%
2	Nurhasni Hasan, Jiafu Cao, Juho Lee, Shwe Phyu Hlaing et al. "Bacteria-Targeted Clindamycin Loaded Polymeric Nanoparticles: Effect of Surface Charge on Nanoparticle Adhesion to MRSA, Antibacterial Activity, and Wound Healing", Pharmaceutics, 2019 Publication	1%
3	Verônica Ferrari Cervi, Camila Parcianello Saccol, Marcel Henrique Marcondes Sari, Carolina Cristóvão Martins et al. "Pullulan film incorporated with nanocapsules improves pomegranate seed oil anti-inflammatory and antioxidant effects in the treatment of atopic dermatitis in mice", International Journal of Pharmaceutics, 2021 Publication	1%
4	Submitted to Sierra College Student Paper	1%
	Submitted to Columbia University	

5	Student Paper	1 %
6	docksci.com Internet Source	1 %
7	www.ncbi.nlm.nih.gov Internet Source	1 %
8	Jin-Wook Yoo, Hasan Nurhasni, Jiafu Cao, Moonjeong Choi, Il Kim, Bok Luel Lee, Yunjin Jung. "Nitric oxide-releasing poly(lactic-co-glycolic acid)-polyethylenimine nanoparticles for prolonged nitric oxide release, antibacterial efficacy, and in vivo wound healing activity", International Journal of Nanomedicine, 2015 Publication	1 %
9	www.mcst.es Internet Source	1 %
10	www.researchgate.net Internet Source	1 %
11	Moonjeong Choi, Nurhasni Hasan, Jiafu Cao, Juho Lee, Shwe Phyu Hlaing, Jin-Wook Yoo. "Chitosan-based nitric oxide-releasing dressing for anti-biofilm and in vivo healing activities in MRSA biofilm-infected wounds", International Journal of Biological Macromolecules, 2020 Publication	1 %

12	www.mdpi.com Internet Source	1 %

Exclude quotes	On	Exclude matches	< 1%
Exclude bibliography	On		